INTERNATIONAL JOURNAL OF CLIMATOLOGY
Int. J. Climatol. **30**: 972–979 (2010)
Published online 20 August 2009 in Wiley InterScience
(www.interscience.wiley.com) DOI: 10.1002/joc.2000

RMetS
Royal Meteorological Society

Temperature reconstruction from tree-ring maximum density of Balfour spruce in eastern Tibet, China

Lily Wang,[a,b]* Jianping Duan,[a,c] Jin Chen,[a,d] Lei Huang[e] and Xuemei Shao[a,b]

[a] *Institute of Geographical Sciences and Natural Resources Research, CAS. 11A Datun Road, Beijing 100101 China*
[b] *Institute of Tibetan Plateau Research, CAS. Beijing, 100085 China*
[c] *Graduate University of Chinese Academy of Sciences, Beijing 100049, China*
[d] *Institute of Vertebrate Paleontology and Paleoanthropology, Chinese Academy of Sciences, Beijing 100044, China*
[e] *National Climate Center, CMA. Beijing 100081 China*

ABSTRACT: Wood from Balfour spruce [*Picea likiangensis var. balfouriana* (Rehd. et Wils.)] was collected at three sites in eastern Tibet. Maximum latewood densities (MXD) were measured by X-ray densitometry; individual series were first cross dated and then combined to form a standard chronology. This chronology was significantly correlated with late summer temperatures on the eastern Tibetan Plateau. It was used to reconstruct the August–September mean temperature for the period 1695–2000 A.D., and it explained the 63.5% of the total temperature variance. Wavelet analysis of the reconstructed temperature series suggested the existence of a 20-year climatic cycle during the period 1800–1860 and a ~50-year cycle at the beginning of the twentieth century. Copyright © 2009 Royal Meteorological Society

KEY WORDS Balfour spruce; maximum latewood density; temperature reconstruction; wavelet analysis; eastern Tibet

Received 20 June 2008; Revised 6 July 2009; Accepted 20 July 2009

1. Introduction

One of the immense geomorphic features on Earth, the Tibetan Plateau, affects macro-scale atmospheric circulation and global climate. Consequently, the climate history of the Tibetan Plateau is an important component in the reconstruction of the Earth's climate history. Several tree-ring chronologies, as climatic proxy records, have been developed from the Tibetan Plateau in recent decades. For example, Shao and Fan (1999) reconstructed the winter mean minimum temperature from 1650 to 1994 with *Picea balfouriana*; Gou *et al*. (2006) presented summer maximum temperatures from 1230 to 2000 using *Juniperus przewalskii*; and Huang and Zhang (2007) rebuilt spring precipitation (May–June) from A.D. 1322 to 2001 with *Sabina przewalskii*. A temperature reconstruction of 379 years was established with Balfour spruce in the source region of the Yangtze River on the Tibetan Plateau by Liang *et al*. (2008). These climate reconstructions make it possible to describe the climate history of the Tibetan Plateau (Garfin *et al*., 2005). However, compared to other continents, such as Europe and North America, the number of tree-ring investigation sites from Asia, and from the Tibetan plateau, in particular, is low. More chronologies are needed to interpret the past climate variability over long temporal and large spatial scales.

Balfour spruce (*Picea likiangensis var balfouriana* (Rehd. et Wils)) is one of the dominant species on the eastern Tibetan Plateau (Chen, 1988). Tree-ring parameters of Balfour spruce, especially the maximum latewood density (MXD), responded very well to temperature during the growing season (Bräuning and Mantwill, 2004). This study presents an August–September temperature reconstruction from the standard chronology of Balfour spruce maximum density, obtained from three sites in eastern Tibet. We also applied wavelet transform analysis to examine the oscillation patterns of the cycle, both in static and dynamic types, and in the occurring period and intensity, which were contained in the reconstructed chronology. This may indicate the potential periodicities of El Niño, of solar activity or of Pacific decadal oscillation (Mantua, 2002; Yang and Zhang, 2003; Huang *et al*., 2004; Moberg *et al*., 2006), for which no study related to Tibetan Plateau has yet been reported.

2. Data and methods

2.1. Study area

Zuogong and Mangkang are located in the Hengduan mountain range in the eastern part of the Tibetan Plateau. The region is intensively dissected by deep gorges of three rivers: Jinshajiang (Jantse Kiang), Lancangjiang (Mekong) and Nujiang (Salween). The topography is characterized by extremely steep high-mountain physiognomy (Figure 1). The climate is mainly influenced by the southwest Asian monsoon. Temperature and precipitation

* Correspondence to: Lily Wang, Institute of Geographical Sciences and Natural Resources Research, CAS. 11A Datun Road, Beijing 100101 China. E-mail: lilywang15@yahoo.ca; wangll@igsnrr.ac.cn

vary spatially according to topography. Records from the meteorological station in Changdu (31°04′N, 96°58′E, 3275 m a.s.l.) show that the 1954–2008 mean annual precipitation is about 482 mm and the mean annual temperature is 7.6 °C (Figure 2). Balfour spruce is the dominant species, sporadically accompanied by Flaky fir (*Abies squamata* Masters). Changdu is located upstream of Lancangjiang, which is less deeply incised than the other two valleys. Spruce forests are distributed only on shady slopes with northern aspects.

The available local meteorological instrumental records cover a very short period for calibrating tree growth with climate (record spans of three local stations are 1991–2000, 1978–2000 and 1954–2000), and the meteorological stations in this region are generally located along the valleys. In order to emphasize the spatial representation, we used grid temperature and precipitation data, averaged from the five grid sets located within the sampling area (Figure 1) collected by New *et al*. (2000). The correlation coefficients between grid data and available instrumental records (51 years) from local weather stations were 0.993 (monthly temperature) and 0.947 (monthly precipitation).

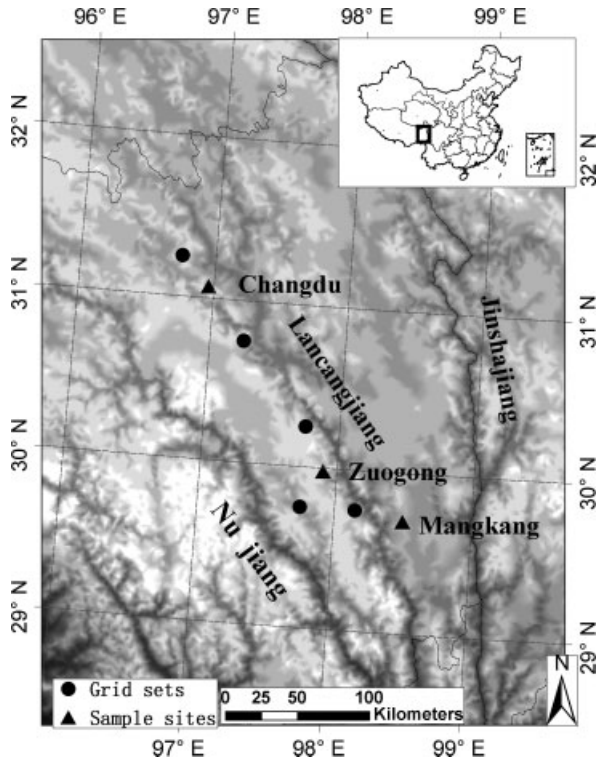

Figure 1. Locations of the sample sites and grid sites.

2.2. Sample collection

Three tree-line Balfour spruce sites with little evidence of fire or human disturbance in the eastern part of the Tibetan Plateau were chosen (Figure 1). Between twenty-one and twenty-five trees were selected at each site, and, from each tree, two increment cores were sampled (Table I). All the sampling sites were at 4150–4500 m elevation a.s.l.; on eastern slopes, they were with an inclination of 30–37°.

2.3. Data analysis

Tree-ring samples were prepared for the densitometric analysis (Lenz *et al*., 1976; Schweingruber *et al*., 1988). Resin was extracted with 95% alcohol for 48 h. Cores were cut into 1.0-mm-thin sections with a twin-blade DENDROCUT, with the angles vertical to the wood fiber, adjusted by a DENDROSCOPE. The thin wood sections were then put into a constant-temperature-and-humidity room for at least 2 h before X-ray photography was taken in the same room. The grey-scale variations of the X-ray film were then measured by the DENDRO2003 instrument. We used maximum latewood density in this study. The COFECHA (Holmes, 1983) program was used for cross dating, and was verified with thin wood sections when inconsistencies appeared. Detrending was carried out with 80-year smoothing splines with ARSTAN

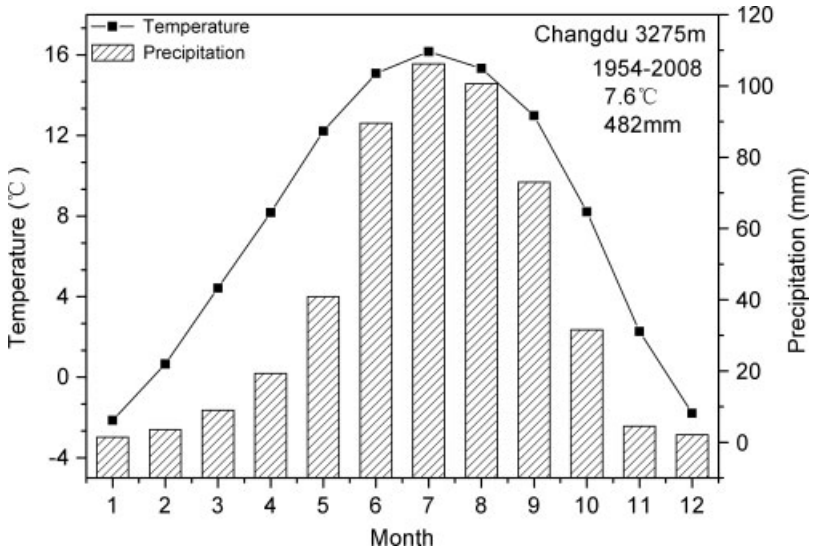

Figure 2. Climate diagram for the meteorological station in Changdu in eastern Tibet.

Table I. Information about the sampling sites and grid sets in eastern Tibet.

Sites	Latitude	Longitude	Elevation	Time span	Years	Trees(cores)
Changdu	31°04′N	96°58′E	4150	1688–2000	313	21(39)
Mangkang	29°42′N	98°30′E	4350	1622–2000	384	23(42)
Zuogong	29°59′N	97°54′E	4500	1510–2000	491	25(45)
Grid set 1	29.75 °N	98.25 °E	–	1950–2000	51	–
Grid set 2	29.75 °N	97.75 °E	–	1950–2000	51	–
Grid set 3	30.25 °N	97.75 °E	–	1950–2000	51	–
Grid set 4	30.75 °N	97.25 °E	–	1950–2000	51	–
Grid set 5	31.25 °N	96.75 °E	–	1950–2000	51	–

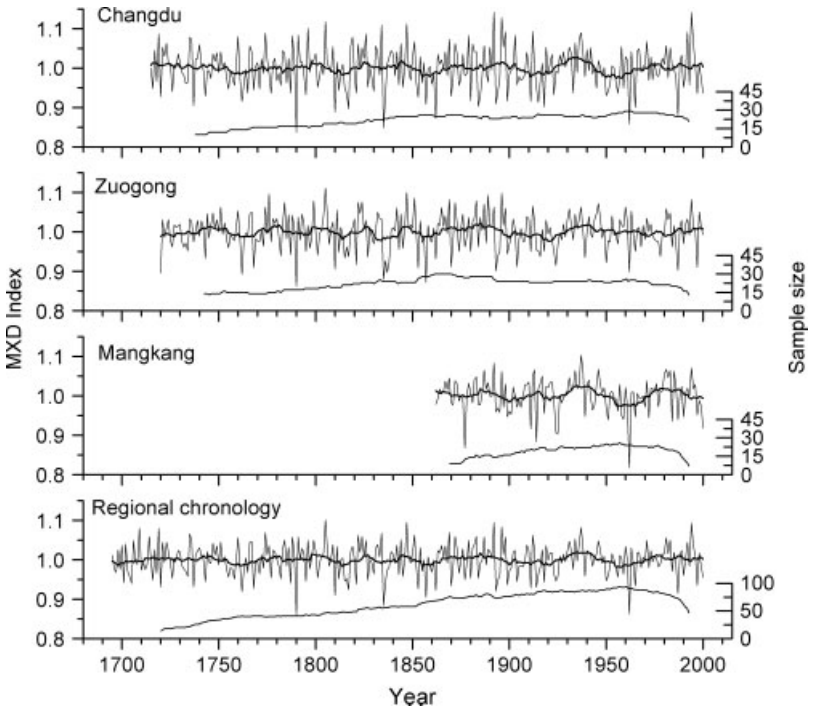

Figure 3. MXD standard chronologies from three sites(Changdu, Zuogong and Mangkang) and the regional chronology with 15-year smoothing (thick line) and sample depth. The beginning year with EPS <0.85.

version August 2006 software, (Cook, 1985). Such a detrending method allows to maximize the common signals among individual tree-ring series and it can reveal the best correlation with climate factors.

We combined all of the MXD series from the three sites to one standard chronology (Figure 3; Table II). Pearson correlation and partial correlation were employed to test the relationship between the MXD chronology and temperature and precipitation from the grid data. We reconstructed August–September temperatures based on the MXD chronology. Owing to the short period of the available climate series, cross verification (leave-one-out) was used to verify the validity of the derived temperature reconstruction (Table III).

2.4. Wavelet analysis

Wavelet analysis can give information about the time evolution of the spectral properties of a quantity. Its use is now becoming increasingly more common in climatology (Oh *et al*., 2003). The potential value of this method is supported by several recently published studies in the field of atmospheric sciences (Torrence and Compo, 1998; Aydin and Markus, 2000). In China, several reports on precipitation analysis have been also applied this technique (Zhang *et al*., 2003; Lu *et al*., 2004; Yu and Sun, 2004).

We uploaded the reconstructed temperature series to an interactive program on a wavelet website (http://paos.colorado.edu/research/wavelets/) for calculating the oscillations cycles along with time.

3. Results

The three sites of MXD chronologies and the combined MXD chronology are presented in Figure 3. High correlation was found between the MXD standard chronology and August–September temperature (Figure 4). It was

Table II. Statistics for the regional MXD standard chronology.

Time span	Corr. between trees	Auto. correlation	Std. deviation	Signal-to-noise ratio	Expressed pupulation signal	SSS[a] >0.85
1510–2000	0.265	0.038	0.122	12.06	0.923	1695–2000

[a] SSS means subsample signal strength

Table III. Statistics of the leave-one-out calibration results for the common period 1950–2000.

Period	R	R^2	R^2_{adj}	F	r	Sign test	Pmt	RE
1950–2000	0.801	0.642	0.635	87.8[a]	0.765	38/13[a]	3.49[a]	0.58

R is correlation coefficient; $\mathbf{R^2}$ and $\mathbf{R^2_{adj}}$ are coefficients of determination and adjusted coefficients of determination of regression analysis; **r** is the correlation coefficient between the recorded data and the leave-one-out-derived estimates. **Pmt** is the product mean test. **Sign test** is sign of paired observed and estimated departures from their mean on the basis of the number of agreement/disagreements; **F** is the F statistic for the statistical significance of the regression models; **RE** is the reduction of error, any positive value indicates there is some sense in the reconstruction (Fritts, 1976).
[a] Significant at $p<0.01$.

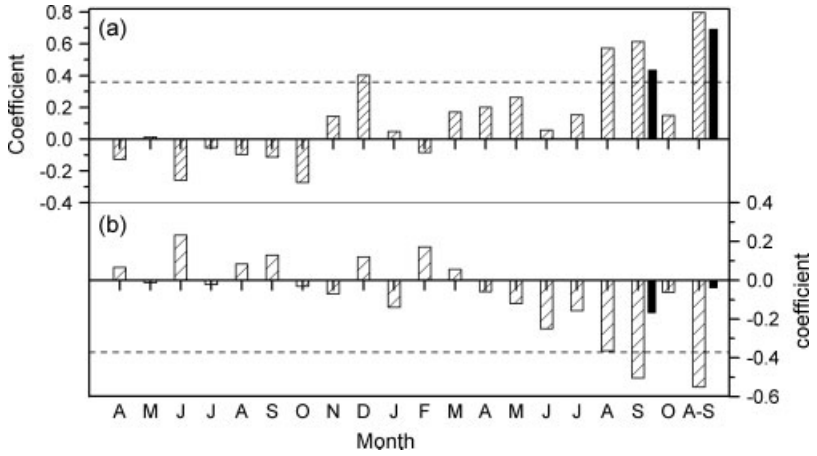

Figure 4. Correlation coefficients between the regional chronology and the grid sets temperature(a) and precipitation (b) from previous April to current October and August–September. White bars are Pearson correlation coefficients, black bars are partial coefficients; horizontal dotted lines indicate statistical significance of 0.01.

positively correlated with the monthly mean temperature in August and September at the 0.01 significance level. Although the chronology was significantly negatively correlated with monthly precipitation of September, partial correlation demonstrated that the coincident variation of MXD was controlled by temperature (Bräuning and Mantwill, 2004). The temperature in previous Decembers was also significantly correlated with the maximum tree-ring density.

The regression and verification test results for the reconstruction of temperature (August–September) are shown in Table III with leave-one-out cross validation, the positive value of the reduction of error (RE) statistic, the results of the product mean test and the sign test indicating the validity of the reconstruction (Michaelsen, 1987). As can be seen in Figure 5, the reconstructed temperature fits very well with the original temperature curve, except for some extraordinary high value points.

A 15-year-smoothing curve of the reconstructed MXD (Figure 6) shows obvious warm periods during 1864–1899 and 1927–1945. Cold periods occurred during 1752–1772 and 1900–1927. Extremely warm summer temperatures occurred during the years 1805, 1847, 1892, 1896, 1937 and 1994; and singularities for low temperature summers were 1762, 1790, 1810, 1836, 1857, 1893, 1962 and 1987.

3.1. Wavelet analysis

The Morlet wavelet transform from temperature reconstruction presented different periodicities, as shown in Figure 7. High-frequency cycles were not detected by the wavelet analysis in this study. This is possibly because this method is not suitable for high-frequency cycle analysis. Therefore, we have focused on decadal and multi-decadal timescales in this study. Cycles of approximately 20 and 50 years of low-frequency tendency were apparent in the reconstructed summer temperatures (Figure 6). The

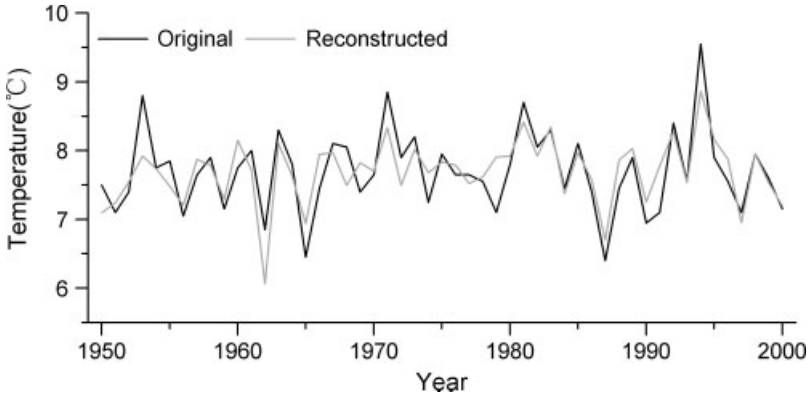

Figure 5. Comparison of the actual (black line) and reconstructed (grey line) August–September temperature.

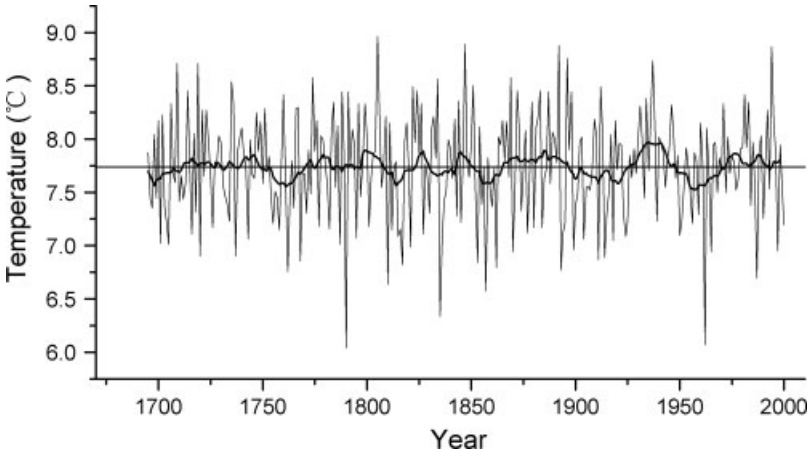

Figure 6. Reconstructed August–September temperature from MXD with 15-year smoothing (thick line).

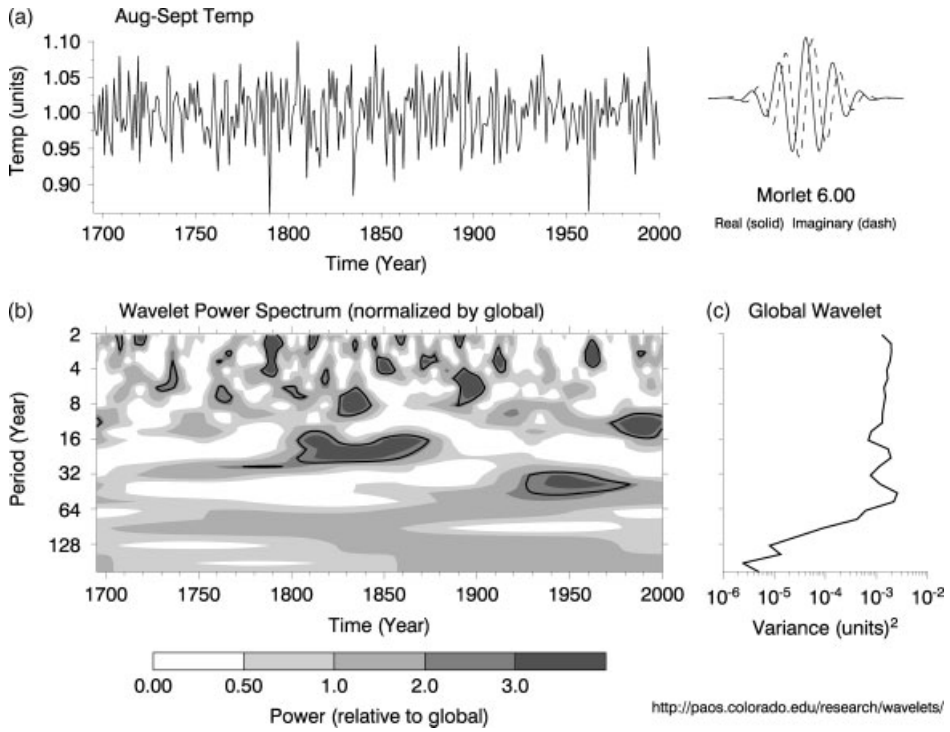

Figure 7. (a) 8–9 Temperature (b) The wavelet power spectrum. The power has been scaled by the global wavelet spectrum (at right). Black contour is the 10% significance level, using the global wavelet as the background spectrum. (c) The global wavelet power spectrum.

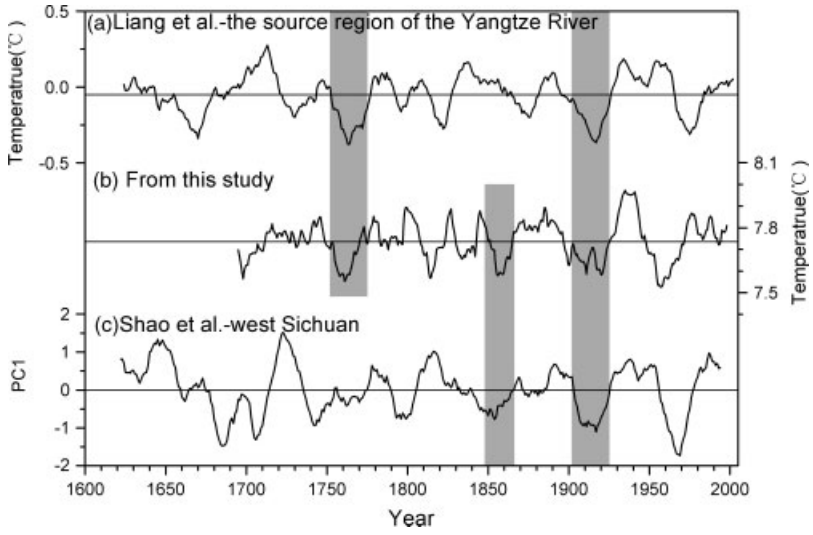

Figure 8. Graphical comparison between the August–September temperature reconstructed in this study and the other two tree-ring records. (a) Mean summer minimum temperature reconstructed in the source region of the Yangtze Revier (Liang *et al*., 2008); (b) August–September temperature reconstructed from this study; (c) first principal component (PC1) of the four tree-ring width chronologies in west Sichuan on the eastern Tibetan Plateau (Shao and Fan, 1999). The thick curves are smoothed values with a 15-year adjacent average and the horizontal lines are the long-term means.

strongest periods for a 20-year cycle appeared around the period 1800–1860, as can also be seen in Figure 3 from a sine-like pattern of the smoothed regional chronology. A ∼50-year cycle exists in the twentieth century.

4. Discussion

The maximum latewood density at the upper tree-line sites is positively correlated with the temperature of the growing season (Briffa *et al*., 1988; Schweingruber *et al*., 1991; Luckman *et al*., 1997). In Arctic regions, the highest correlation may occur in August and September, indicating that this is the most important period for tracheid cell wall thickening (Wang *et al*., 2002). In this study, the synchronized variations responding to August–September temperature suggest that Balfour spruce forests growing at the upper tree-line, above 4000 m altitude, also reflect similar information about climate changes, as observed in records from high latitude regions. Therefore, the Balfour spruce has great potential for estimating temperature variations on a larger spatial scale.

In the temperature reconstruction (Figure 8), cold and warm periods after 1850 were very similar to those found in Chuanxi (29–30 °N; 101 °E) (Shao and Fan, 1999) (Figure 8(c)). The presence of cold decades around 1860s, 1910s and 1960s, and warm decades around 1890s and 1930s, was also reported by Bräuning (2001) and Bräuning and Mantwill (2004). Our reconstruction also agrees with the summer minimum temperature reconstruction on the Tibet Plateau (Liang *et al*. (2008) (Figure 8(a)). The common cold periods of our reconstruction with Liang are around the 1910s and 1760s and the common warm periods are in the1930s, 1890s, 1800s and 1740s. In our reconstruction, the cold year, 1962, was identical to the above-mentioned reconstructions. As historical reports from the Tibetan Plateau are very rare, we compared a study on historical climate data from eastern China. We found that only two cold signal years (1762 and 1893) matched the cold year list in this report (Gong *et al*., 1987). These cold winters either occurred on a large spatial scale or might only have been coincidental events that have not yet been clearly identified.

The worldwide registered cold years in 1816 and 1817 (Filion *et al*., 1986; Lamb, 1995) were also below average in this series. The low temperature signal for 'the year without summer', 1816 and 1817, especially for 1817, was shown in the reconstructed temperature series. In addition, there was no signal in 1992 – another cold year triggered by volcanic activity (Xu, 1995). This cold year has been shown to result in remarkably light rings in over 80% of the spruce trees along the arctic treeline in the northern Quebec province, Canada (Wang *et al*., 2000). An explanation for this finding is that the atmospheric circumfluence distributes volcanic dust from low-latitude sources towards the northwest. Thus, its principal impact is on Europe, North America, and then the polar regions, and it never reaches the Tibetan plateau (Yang *et al*., 2005). The grid climate data used in this study have provided a complementary opportunity for dendroclimatology where instrumental records are lacking or are only very short for remote regions like the Tibetan Plateau.

Cycles of approximately 20 and 50 years existed in the reconstructed summer temperatures (Figure 9). The strongest periods of the 20-year cycle appear around 1800–1860, and the ∼50-year cycle exists in the twentieth century. These two cycles are similar to the Pacific decadal oscillation (PDO) that occurred during the twentieth century (Huang, 2000; Mantua, 2002). PDO

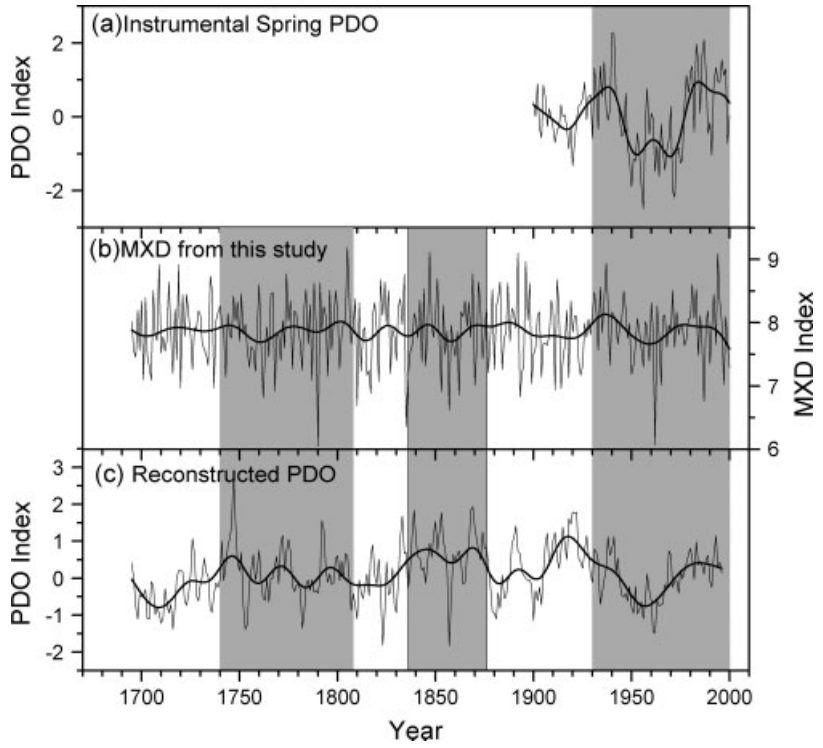

Figure 9. Graphical comparison of the MXD index reconstructed in this study with two PDO indexes: (a) Instrumental spring (March–April–May) PDO index from 1900–2000 (D'Arrigo and Wilson, 2006) and (c) reconstructed PDO index for the past millennium (MacDonald *et al*., 2005).

fluctuations were most energetic in two general periodicities, one from 15–25 years and the other from 50–70 years.

A comparison has been made between our MXD and the two PDO series (Figure 9). A high correlation was found ($r = 0.21$, $p < 0.05$) between August and September temperatures reconstructed in this study and the instrumental spring (March–April–May) PDO index (D'Arrigo and Wilson, 2006), and the two series (Figure 9(a) and (b)) show a rather similar variation trend from 1900 to 2000. A significant correlation ($r = 0.116$, $p < 0.05$) also has been in existence between our MXD and the reconstructed PDO index for the past millennium (MacDonald *et al*., 2005) during 1695–2000, and the reconstructed PDO series indicated that a ~50 to 70 year periodicity is typical for the past 200 years (MacDonald *et al*., 2005), which agrees with our ~50-year cycle in wavelet analysis. As shown in Figure 9, our MXD series also agrees with the reconstructed PDO variation (Figure 9(c)), especially for the periods 1930–2000s, 1830–1870s and 1740–1800s. Thus, the large-scale and distinct expression of the PDO (D'Arrigo and Wilson, 2006) is further supported by our tree-ring data.

Causes for the PDO or for the periodicities in this study are currently unknown. However, these time series analyses offer the possibility of developing macro-scale reconstructions of climate history on different temporal and spatial domains, even though the biological meaning of the oscillations of the recognized cycles is not clear at the moment. Thus far, only a few results derived with these relatively new methods have been reported in dendrochronological research. Further studies are needed to evaluate their applicability in tree-ring research.

5. Conclusions

1. Balfour spruce forests at the tree-line can be used for reconstructing late summer temperatures, both temporally and spatially.
2. The standard chronology of the maximum latewood density from Changdu, Mangkang and Zuogong, in eastern Tibet, can explain 63.5% of the variance in the August–September temperatures.
3. Wavelet analysis showed that intensive variation periods of 20-year frequencies appeared during the period 1800–1860, and ~50-year cycles occurred during the twentieth century. These two cycles are similar to the previously reported Pacific decadal oscillation.

Acknowledgements

This study was supported by National Natural Science Foundation of China, under the grants no. 90 211 018, 30 270 227 and 49 971 079. We thank Zhi-Yong Yin and Achim Bräuning for valuable comments and English improvement. Two anonymous reviewers are also thanked for their suggestions.

References

Aydin N, Markus HS. 2000. Directional wavelet transform in the context of complex Quadrature Doppler signals. *IEEE Signal Processing Letters* **7**(10): 278–280.

Bräuning A. 2001. Climate history of the Tibetan Plateau during the last 1000 years derived from a network of juniper chronologies. *Dendrochronologia* **19**: 127–137.

Bräuning A, Mantwill B. 2004. Increase of Indian Summer Monsoon rainfall on the Tibetan plateau recorded by tree rings. *Geophysical Research Letters* **31**: L24205. DOI 10.1029/2004GL020793.

Briffa KR, Jones PD, Schweingruber FH. 1988. Summer temperature patterns over Europe: a reconstruction from 1759 A.D. based on muximum latewood density indices of conifers. *Quaternary Research* **30**: 36–52.

Chen W. 1988. Forest (IV) in Vegetation of Xizang (Tibet). In *Climate Dynamics*, Vol. 23, Yu B (ed). Science Press: Beijing; 869–881.

Cook ER. 1985. *A Time-series Analysis Approach to Tree-ring Standardization*. Ph.D. thesis, University of Arizona, Tucson, USA.

D'Arrigo R, Wilson R. 2006. On the Asian expression of the PDO. *International Journal of Climatology* **26**: 1607–1617.

Filion L, Payette S, Gauthier L, Boutin Y. 1986. Light rings in subarctic conifers as a dendrochronological tool. *Quaternary Research* **26**(2): 272–279.

Fritts HC. 1976. *Tree Rings and Climate*. Academic Press: London; 567.

Garfin GM, Hughes MK, Yu L, Burns JM, Touchan R, Leavitt SW, An ZS. 2005. Exploratory temperature and precipitation reconstructions from the Qinling Mountains, north-central China. *Tree-Ring Research* **61**(2): 59–72.

Gong G, Zhang P, Zhang J. 1987. *The Cold Winter in 1892–1893 and its Effect*. Vol. 18, Science Press: Beijing; 129–138. Geography Collection (in Chinese).

Gou X, Chen F, Yang M, Jacoby G, Peng J, Zhang Y. 2006. A comparison of tree-ring records and glacier variations over the past 700 years, northeastern Tibetan Plateau. *Annals of Glaciology* **43**: 86–90.

Holmes RL. 1983. Computer-assisted quality control in tree-ring dating and measurement. *Tree-Ring Bulletin* **43**: 69–78.

Huang J. 2000. *Meteorological Statistical Analysis and Forecasting Methods*. China Meteorological Press: Beijing. in Chinese.

Huang L, Shao X, Liang E, Wang L. 2004. Characteristics of millennial tree-ring width variations of Qilian juniper in Shalike Mountain, Qinghai. *Geographical Research* **23**(3): 365–373.

Huang J, Zhang Q. 2007. Tree rings and climate for the last 680 years in Wulan area of northeastern Qinghai-Tibetan Plateau. *Climate Change* **80**(3–4): 369–377.

Lamb HH. 1995. *Climate, History and the Modern World*. Routledge; 141–271.

Lenz O, Schaer E, Schweingruber FH. 1976. Methodische Probleme bei der radiographisch- densitometrischen Bestimmung der Dichte und der Jahrringbreiten von Holz. *Holzforschung* **30**(4): 114–123. Unofficial English title: Methodological problems relative to the measurement of the density and width of growth rings by X-ray densitograms of wood.

Liang E, Shao X, Qin N. 2008. Tree-ring based summer temperature reconstruction for the source region of the Yangtze River on the Tibetan Plateau. *Global and Planetary Change* **61**: 313–320.

Lu H, Zhang F, Liu X, Duce RA. 2004. Periodicity of palaeoclimatic variations recorded by loess-paleosol sequences in China. *Quaternary Science Reviews* **23**(18–19): 1891–1900.

Luckman BH, Briffa KR, Jones PD, Schweingruber FH. 1997. Tree-ring based reconstruction of summer temperatures at the Columbia Icefield, Alberta, Canada, AD 1073–1983. *The Holocene* **7**(4): 375–389.

MacDonald GM, Case RA. 2005. Variations in the pacific decadal oscillation over the past millennium. *Geophysical Research Letters* **32**: L08703. DOI 10.1029/2005GL022478.

Mantua NJ. 2002. The pacific decadal oscillation. *Journal of Oceanography* **58**(1): 35–44.

Michaelsen J. 1987. Cross-validation in statistical climate forecast models. *Journal of Climate and Applied Meteorology* **26**(11): 1589–1600.

Moberg A, Sonechkin DM, Holmgren K, Datsenko NM, Karlén W, Lauritzen SE. 2006. Highly variable Northern Hemisphere temperatures reconstructed from low- and high-resolution proxy data. *Nature* **433**: 613–617.

New M, Hulme M, Jones PD. 2000. Representing twentieth century space–time climate variability: Part II. Development of 1901–1996 monthly grids of terrestrial surface climate. *Journal of Climate* **13**(13): 2217–2238.

Oh H-S, Ammann CM, Naveau P, Nychka D, Otto-Bliesner BL. 2003. Multi-resolution time series analysis applied to solar irradiance and climate reconstruction. *Journal of Atmospheric and Solar-Terrestrial Physics* **65**(2): 191–201.

Schweingruber FH, Bartholin T, Schär E, Briffa KR. 1988. Radio-densitometric-dendroclimatological conifer chronologies from Lapland (Scandinavie) and the Alps (Switzerland). *Boreas* **17**: 559–566.

Schweingruber FH, Briffa KR, Jones PD. 1991. Yearly maps of summer temperatures in western Europe from A.D. 1750 to 1975 and western North America from 1600 to 1982: Results of a radiodensitometrical study on tree rings. *Vegetatio* **92**(1): 5–71.

Shao X, Fan J. 1999. Past climate on west Sichuan plateau as reconstructed from ring-widths of dragon spruce. *Quaternary Sciences* **1**: 81–89. in Chinese.

Torrence C, Compo GP. 1998. A practical guide to wavelet analysis. *Bulletin of the American Meteorological Society* **79**: 61–78.

Wang L, Payette S, Begin Y. 2000. A quantitative definition of light rings in black spruce (Picea mariana) at the Arctic treeline in northern Quebec, Canada. *Arctic, Antarctic, and Alpine Research* **32**: 324–330.

Wang L, Payette S, Begin Y. 2002. Relationships between anatomical and densitometric characteristics of black spruce and summer temperature at tree line in northern Quebec. *Canadian Journal of Forest Research* **32**: 477–486.

Xu Q. 1995. Influences of Pinatubo volcanic clouds on large scale climate in 1992. *Quarterly Journal of Applied Meteorology* **6**: 35–42.

Yang Y, Man Z, Zheng Y. 2005. A serious famine in Yunnan (1815–1817) and the eruption of Tambola Valcano. *Fudan journal (Social Science) (in Chinese)* **1**: 79–85.

Yang HJ, Zhang J. 2003. On the decadal and interdecadal variability in the pacific ocean. *Advances in Atmospheric Sciences* **2**: 173–184.

Yu Z, Sun Z. 2004. Analysis of multi-scale features of tropical pacific ocean see surface temperature. *Journal of Nanjing Institute of Meteorology* **27**: 193–199.

Zhang Q, Cheng G, Yao T, Kang X, Huang J. 2003. A 2,326-year tree-ring record of climate variability on the northeastern Qinghai-Tibetan Plateau. *Geophysical Research Letters* **30**(14): 1–4.

